

Chapter 13

COSY: Quantitative Analysis

Alex D. Bain

Department of Chemistry, McMaster University, Hamilton L8S 4M1, Ontario, Canada

13.1 Introduction	167
13.2 COSY on a Two-Spin System	168
13.3 Larger Spin Systems	175
13.4 Fast Pulsing Artifacts	175
13.5 Conclusions	176
References	176

13.1 INTRODUCTION

The COSY¹ experiment (Figure 13.1) is probably the single most important two-dimensional NMR experiment. The experiment provides a homonuclear chemical shift correlation: if two spins are connected by a scalar coupling, then the COSY spectrum will show a pair of symmetrical cross peaks between the diagonal peaks of two spins (see Chapter 12). Although the SECSY experiment was often used for homonuclear correlation,^{2,3} COSY is the one that has survived. It is the simplest pulse sequence, requires no prior knowledge of the spin parameters, is the easiest to analyze theoretically, provides some of the most useful structural information, and is probably the most widely used 2D experiment. For these reasons, there are several variations on the basic experiment. To begin with,

a 2D experiment is not just a pulse sequence but also the associated phase cycling sequence, so that must be considered. COSY has also been the subject of many theoretical investigations. The information that it provides is often simply qualitative (on what is coupled to what), but it is important to understand the quantitative basis of COSY as well.

A quantitative analysis of COSY is needed to understand the conditions under which the experiment will work. Many spin systems have a variety of coupling constants ranging from large geminal couplings of 15 Hz or more, through typical vicinal couplings of a few Hz, down to long-range couplings of a fraction of a Hz. Under what circumstances will these couplings show up as cross peaks in a COSY? In a complex system, a multiplet will consist of several splittings corresponding to couplings to several different spins. What are the intensity ratios within a multiplet? Do any new frequencies appear in F_1 ? In a COSY cross peak connecting two spins, how does the active coupling (the one between the two spins in question) appear relative to the passive couplings to the other spins in the system? What happens if the flip angles or the phase cycling sequence is changed? What happens if the spin system does not reach equilibrium between pulse sequences? What is the role of phase cycling and quadrature detection? These are just some of the questions that arise from a detailed examination of the COSY experiment.

Understanding the COSY experiment is relatively easy since it is such a simple experiment. The manipulations are straightforward matrix operations

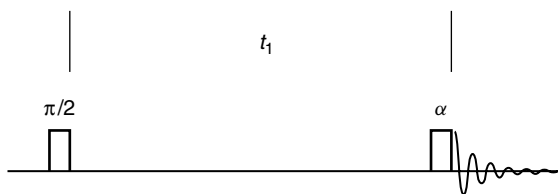


Figure 13.1. COSY pulse sequence. The initial $\pi/2$ pulse excites the spin system which evolves during the regularly-incremented delay t_1 . The second pulse is called the mixing pulse and may have any flip angle, α . For many applications, $\alpha = \pi/2$ or $\alpha = \pi/4$.

and no more difficult than simple spectral analysis. COSY can also serve as a prototype for all multi-dimensional experiments, since it illustrates many of the principles seen in more complex techniques. In this chapter, we discuss a simple COSY experiment on a two-spin system in detail. This will cover many of the points raised in the previous paragraphs and serve as a basis for a discussion of more complex systems.

13.2 COSY ON A TWO-SPIN SYSTEM

The simplest system has two spins $1/2$, labeled A and B, with Larmor frequencies of ν_A and ν_B . These spins are scalar-coupled with a coupling constant of J , so the spectrum consists of two doublets. Figure 13.2 shows the energy levels and the allowed transitions. We assume the coupling is weak, so that all four lines

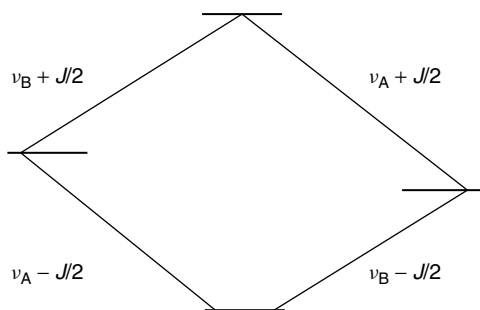


Figure 13.2. The energy levels of a two spin- $1/2$ system and the allowed single quantum transitions. The two spins, labeled A and B, have Larmor frequencies ν_A and ν_B , and are scalar coupling with a coupling constant of J .

in the spectrum have the same intensity. These four lines in the spectrum correspond to density matrix elements which oscillate at these four frequencies. The four lines will all mix with each other in a COSY, so there will be 16 lines in the two-dimensional spectrum. We can study the frequencies, intensities, and phases of these 16 lines by following the modulation of the basic spectrum in the 2D experiment.

13.2.1 Basic Theory

For any line in a spectrum at frequency ν (in the rotating frame of reference), there are two associated oscillating density matrix elements. These can be thought of as the x and the y magnetization, or as two counter-rotating magnetizations rotating at the appropriate frequency. We choose the latter picture, and denote the two density matrix elements as $|+\nu\rangle$ and $|-\nu\rangle$. Any coherence associated with the density matrix element $|+\nu\rangle$ will evolve during a delay time, t , as $e^{+i\nu t}$. The terms positive and negative, strictly speaking, refer to the coherence level, a quantum number associated with each coherence. Of course, the frequencies may themselves be either positive or negative with respect to the carrier frequency, and coupling constants may have either sign. This provides the mathematical description of the rotating magnetization.

13.2.2 Excitation and Evolution

The COSY experiment consists of an excitation pulse, an evolution time t_1 , a mixing pulse, and then detection. We will assume that the spin system is in equilibrium at the start of the sequence. The $\pi/2$ excitation pulse in Figure 13.1 creates coherence corresponding to the four lines in the spectrum, which we will allow to have unit intensity, for simplicity. There will be four positively-rotating elements and four negative ones. These will evolve during the evolution time, so that at the end of t_1 the positively-rotating density matrix elements are given by equation (13.1).

$$\left. \begin{aligned} |\nu_A + J/2\rangle &= e^{+i(\nu_A + J/2)t_1} \\ |\nu_A - J/2\rangle &= e^{+i(\nu_A - J/2)t_1} \\ |\nu_B + J/2\rangle &= e^{+i(\nu_B + J/2)t_1} \\ |\nu_B - J/2\rangle &= e^{+i(\nu_B - J/2)t_1} \end{aligned} \right\} \quad (13.1)$$

Similarly, the elements at negative frequency are given by equation (13.2).

$$\left. \begin{aligned} | -\nu_A - J/2) &= e^{-i(\nu_A + J/2)t_1} \\ | -\nu_A + J/2) &= e^{-i(\nu_A - J/2)t_1} \\ | -\nu_B - J/2) &= e^{-i(\nu_B + J/2)t_1} \\ | -\nu_B + J/2) &= e^{-i(\nu_B - J/2)t_1} \end{aligned} \right\} \quad (13.2)$$

The mixing pulse in the COSY experiment ends the evolution. The effect of this pulse is the key to the experiment, determining what frequencies will appear in F_1 and with which intensities and phases. In general, the calculation of the effect of a pulse with general flip angle and phase on a general spin system is quite complex and beyond the scope of this chapter. The simple evolution during a delay, as above, is relatively easy to picture, but the effect of a pulse is the subject of several theoretical descriptions for pulse NMR.^{4,5}

13.2.3 Frequencies in a COSY Spectrum

The mixing pulse should not introduce any new frequencies into the spectrum, so that any frequency that appears in F_1 in a COSY spectrum should also be there in the simple 1D spectrum. The 1D spectrum may be quite complex, but regardless of how complicated the spectrum is no new frequencies will be present in F_1 . The principal assumption behind this sweeping statement is that the spin system should be in equilibrium before the pulse sequence starts. This assumption is seldom true in routine practice of COSY. Artifacts⁶ are quite common in COSY spectra, but these artifacts are usually simple multiples of the genuine F_1 frequencies. A more detailed discussion of these artifacts and strategies to suppress them is given later.

The reason that no new frequencies are introduced is that only single quantum transitions are excited and detected. A nonselective pulse acting on any spin system in equilibrium will produce only single quantum transitions: the normal equilibrium spectrum. If we ignore relaxation effects, the single quantum transitions will evolve only amongst themselves during the delay. Even though the mixing pulse may create all orders of multiple quantum coherence, only single quantum coherence can be detected directly. In fact, quadrature detection implies that only one of the two senses of precession will be detected, so that only one of the two sets, equation

(13.1) or equation (13.2), will be observed. Hence, a two-pulse experiment like COSY acting on a spin system in equilibrium will only involve single quantum transitions.

The fact that frequencies in F_2 become frequencies in F_1 means that there is a symmetry to the COSY spectrum.⁷ Cross peaks should always occur as symmetrically placed pairs about the main diagonal. This is a very powerful result. It can help us in sorting out genuine cross peaks from artifacts, since artifacts are very seldom symmetrical.

13.2.4 The Mixing Pulse

In the COSY experiment, where we are dealing only with single quantum coherence, the effect of the pulse is relatively simple. For a weakly coupled spin system subjected to pulses whose flip angles and phases are multiples of $\pi/2$, product operator methods are the most popular approach. In this chapter, we will take a more general approach in order to see what happens when we go beyond the simple systems. The possible frequencies of lines in F_1 are defined by the one-dimensional spectrum for all types of spin systems and flip angles/phases of the mixing pulse. We must calculate the intensities and phases of the lines under these circumstances.

The effect of a pulse is best handled by using the angular momentum properties of the spin system. A pulse is equivalent to a rotation of the frame of reference and angular momentum functions, or spherical tensors, provide a natural basis for describing what happens during a rotation. For any spin system we can convert to a spherical tensor basis, and then the effect of a pulse is simply given by a Wigner matrix element, independent of the details of the spin system.

Among the single quantum transitions, the pulse can take a positive frequency and mix it with the other positive frequencies; it can take a positive frequency, reverse its sense of precession and mix it with the negative frequencies; or it can put a rotating magnetization back up on the z axis. We will ignore the magnetization put back along z and then treat each of the two other cases separately.

The matrix that takes the positive frequencies into the negative frequencies is given by equation (13.3). Equation (13.4) gives the matrix which takes the positive frequencies into themselves.

$$\begin{bmatrix} \frac{1}{2} \sin^2 \frac{\alpha}{2} (1 + \cos \alpha) & \frac{1}{2} \sin^2 \frac{\alpha}{2} (1 - \cos \alpha) & \frac{\sin^2 \alpha}{4} & \frac{-\sin^2 \alpha}{4} \\ \frac{1}{2} \sin^2 \frac{\alpha}{2} (1 - \cos \alpha) & \frac{1}{2} \sin^2 \frac{\alpha}{2} (1 + \cos \alpha) & \frac{-\sin^2 \alpha}{4} & \frac{\sin^2 \alpha}{4} \\ \frac{\sin^2 \alpha}{4} & \frac{-\sin^2 \alpha}{4} & \frac{1}{2} \sin^2 \frac{\alpha}{2} (1 + \cos \alpha) & \frac{1}{2} \sin^2 \frac{\alpha}{2} (1 - \cos \alpha) \\ \frac{-\sin^2 \alpha}{4} & \frac{\sin^2 \alpha}{4} & \frac{1}{2} \sin^2 \frac{\alpha}{2} (1 - \cos \alpha) & \frac{1}{2} \sin^2 \frac{\alpha}{2} (1 + \cos \alpha) \end{bmatrix} \quad (13.3)$$

$$\begin{bmatrix} \frac{1}{2} \cos^2 \frac{\alpha}{2} (1 + \cos \alpha) & \frac{1}{2} \cos^2 \frac{\alpha}{2} (1 - \cos \alpha) & \frac{-\sin^2 \alpha}{4} & \frac{\sin^2 \alpha}{4} \\ \frac{1}{2} \cos^2 \frac{\alpha}{2} (1 - \cos \alpha) & \frac{1}{2} \cos^2 \frac{\alpha}{2} (1 + \cos \alpha) & \frac{\sin^2 \alpha}{4} & \frac{-\sin^2 \alpha}{4} \\ \frac{-\sin^2 \alpha}{4} & \frac{\sin^2 \alpha}{4} & \frac{1}{2} \cos^2 \frac{\alpha}{2} (1 + \cos \alpha) & \frac{1}{2} \cos^2 \frac{\alpha}{2} (1 - \cos \alpha) \\ \frac{\sin^2 \alpha}{4} & \frac{-\sin^2 \alpha}{4} & \frac{1}{2} \cos^2 \frac{\alpha}{2} (1 - \cos \alpha) & \frac{1}{2} \cos^2 \frac{\alpha}{2} (1 + \cos \alpha) \end{bmatrix} \quad (13.4)$$

These equations are valid for any flip angle, α , of the mixing pulse applied to a weakly coupled spin system. For $\alpha = \pi$, note that the matrix in equation (13.4) vanishes completely and the only elements in equation (13.3) that survive are the ones that connect the two lines in each doublet together: elements (1,2), (2,1), (3,4), and (4,3). This is the mixing in the multiplets that gives rise to J-modulation in spin echoes (see Chapter 11).

The simple COSY experiment involves a $\pi/2$ mixing pulse, so we must include the effects of both matrices. Since we detect only one sense of precession, say the positive one, we need only calculate the coherences that contribute to that set. Therefore, to describe what the mixing pulse does, we multiply the coherences in equation (13.2) by the matrix in equation (13.3)—these are the coherences with a negative coherence level going into the positives. The result of this is given in equation (13.5).

$$\begin{aligned} |v_A + J/2\rangle &= \frac{1}{4} [e^{-i(v_A + J/2)t_1} \\ &\quad + e^{-i(v_A - J/2)t_1} + e^{-i(v_B + J/2)t_1} - e^{-i(v_B - J/2)t_1}] \\ |v_A - J/2\rangle &= \frac{1}{4} [e^{-i(v_A + J/2)t_1} \\ &\quad + e^{-i(v_A - J/2)t_1} - e^{-i(v_B + J/2)t_1} + e^{-i(v_B - J/2)t_1}] \\ |v_B + J/2\rangle &= \frac{1}{4} [e^{-i(v_A + J/2)t_1} \\ &\quad - e^{-i(v_A - J/2)t_1} + e^{-i(v_B + J/2)t_1} + e^{-i(v_B - J/2)t_1}] \\ |v_B - J/2\rangle &= \frac{1}{4} [-e^{-i(v_A + J/2)t_1} \\ &\quad + e^{-i(v_A - J/2)t_1} + e^{-i(v_B + J/2)t_1} + e^{-i(v_B - J/2)t_1}] \end{aligned} \quad (13.5)$$

Added to this is the result of applying the matrix in equation (13.4) to the coherences in equation (13.1). The contribution of the positive coherences is given by equation (13.6).

$$\begin{aligned} |v_A + J/2\rangle &= \frac{1}{4} [e^{+i(v_A + J/2)t_1} \\ &\quad + e^{+i(v_A - J/2)t_1} - e^{+i(v_B + J/2)t_1} + e^{+i(v_B - J/2)t_1}] \\ |v_A - J/2\rangle &= \frac{1}{4} [e^{+i(v_A + J/2)t_1} \\ &\quad + e^{+i(v_A - J/2)t_1} + e^{+i(v_B + J/2)t_1} - e^{+i(v_B - J/2)t_1}] \\ |v_B + J/2\rangle &= \frac{1}{4} [-e^{+i(v_A + J/2)t_1} \\ &\quad + e^{+i(v_A - J/2)t_1} + e^{+i(v_B + J/2)t_1} + e^{+i(v_B - J/2)t_1}] \\ |v_B - J/2\rangle &= \frac{1}{4} [e^{+i(v_A + J/2)t_1} \\ &\quad - e^{+i(v_A - J/2)t_1} + e^{+i(v_B + J/2)t_1} + e^{+i(v_B - J/2)t_1}] \end{aligned} \quad (13.6)$$

The final result is the sum of equations (13.5) and (13.6), to give the expressions in equation (13.7).

$$\begin{aligned} |v_A + J/2\rangle &= \frac{1}{4} [\cos(v_A + J/2)t_1 \\ &\quad + \cos(v_A - J/2)t_1 - \sin(v_B + J/2)t_1 \\ &\quad + \sin(v_B - J/2)t_1] \\ |v_A - J/2\rangle &= \frac{1}{4} [\cos(v_A + J/2)t_1 \\ &\quad + \cos(v_A - J/2)t_1 + \sin(v_B + J/2)t_1 \\ &\quad - \sin(v_B - J/2)t_1] \\ |v_B + J/2\rangle &= \frac{1}{4} [-\sin(v_A + J/2)t_1 \\ &\quad + \sin(v_A - J/2)t_1 + \cos(v_B + J/2)t_1 \\ &\quad + \cos(v_B - J/2)t_1] \\ |v_B - J/2\rangle &= \frac{1}{4} [\sin(v_A + J/2)t_1 \\ &\quad - \sin(v_A - J/2)t_1 + \cos(v_B + J/2)t_1 \\ &\quad + \cos(v_B - J/2)t_1] \end{aligned} \quad (13.7)$$

This is the modulation of the lines resulting from the simple pulse sequence in Figure 13.1. The modulation is a cosine modulation, with the diagonal peaks (the peaks due to mixing within a multiplet) $\pi/2$ out of phase with the cross peaks, and the two cross peaks of opposite sign. Since this is a cosine modulation, a real Fourier transform (as distinct from a complex one) will extract the data.

Depending on the phase correction used, the diagonal peaks will be dispersion in both dimensions and the cross peaks will be absorption in both F_1 and F_2 . This is the basic COSY experiment (note that no phase cycling was done), but there are problems with it and many variations have been developed.

13.2.5 Different Types of COSY

The different types of COSY experiment generally do not change the basic pulse sequence in Figure 13.1, but rather vary the associated phase cycling scheme and the way that the data are transformed. One of the problems is that the cosine modulation in equation (13.7) cannot distinguish between positive and negative frequencies, so quadrature detection in F_1 is not possible. In itself this is not too much of a problem, since quadrature detection in F_1 does not give any signal to noise ratio advantage.⁸ However, the lack of quadrature detection in F_1 in a homonuclear experiment prevents its use in F_2 where there is an advantage to its use.

Historically, the first solution to the problem was to use a complex FT, that is to use $e^{i\omega t}$ in the transform rather than $\cos(\omega t)$. When applied to the data in equation (13.7), this gives peaks at both positive and negative frequencies, since $\cos(\omega t) = 1/2(e^{i\omega t} + e^{-i\omega t})$. These peaks were called P-type and N-type peaks.² One or other of these can be removed by phase cycling — repeating the same pulse sequence, but with different phases in the pulses.^{9,10} This removes (usually) the positive-to-positive transfer given by equation (13.6), so that the data have a complex modulation given by equation (13.5). The disadvantage of this method is that the lineshapes no longer have a pure phase, but rather a so-called phase-twist in which the phase in one dimension changes as one moves across the other dimension. Figure 13.3 shows the phase-twist lineshape. This phase problem can be circumvented by the use of pseudo-echo, or sine-bell type apodization functions, and a magnitude calculation rather than a phase correction after the 2D FT. This form of the COSY experiment is very popular and very simple to set up and process.

Figures 13.4, 13.5, 13.6, 13.7, and 13.8 show typical results from such an experiment on the molecule serine. Serine is a convenient sample for experimenting with 2D NMR since the chemical shifts of the

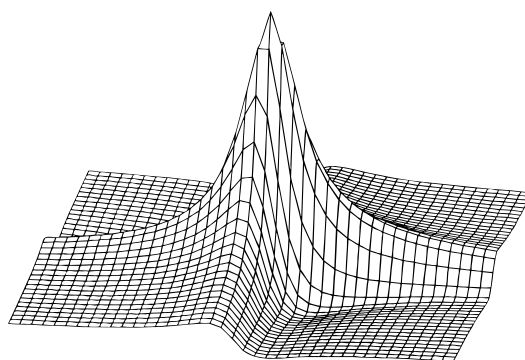


Figure 13.3. The so-called “phase-twist” lineshape often encountered in COSY spectra. In the center of the line the lineshape is pure absorption, but in the wings in each dimension it becomes more dispersion-like.

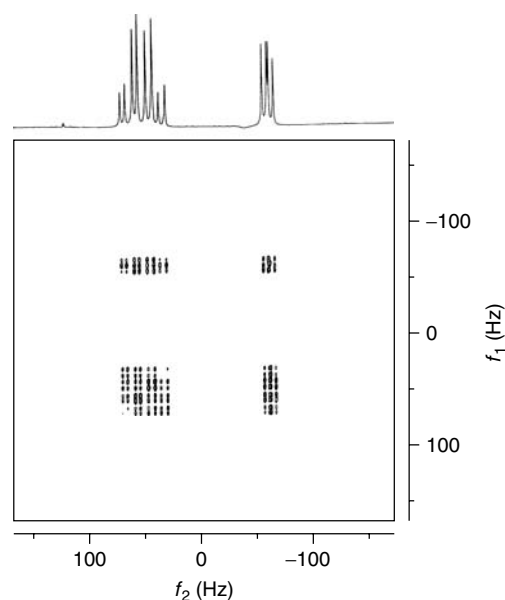


Figure 13.4. Magnitude calculation COSY on serine, $\text{NH}_2\text{CH}(\text{CH}_2\text{OH})(\text{COOH})$, in D_2O at pH 10 at a spectrometer frequency of 300 MHz. The mixing pulse had a flip angle of $\pi/2$. The raw data consisted of 256 FIDs of 1 k data points, which were Fourier-transformed using an unshifted sine-bell squared apodization in both dimensions. The spectral width in both dimensions was 338 Hz, giving a digital resolution of 0.66 Hz per point. The α proton in serine is at low frequency and the two β protons, β and β' , are 0.339 and 0.410 ppm to high frequency at this pH. The measured coupling constants are $J_{\alpha\beta} = 5.9$ Hz, $J_{\alpha\beta'} = 4.3$ Hz, and $J_{\beta\beta'} = -11.2$ Hz.

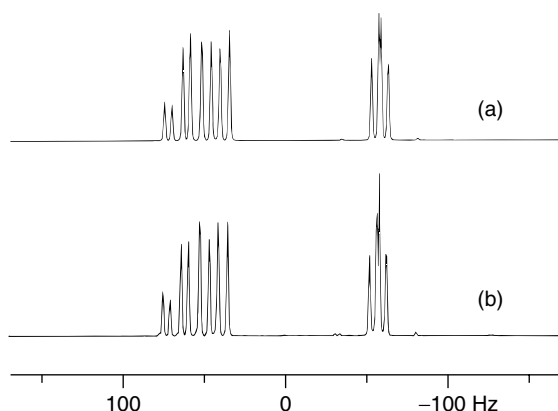


Figure 13.5. Plot of a row from the data matrix in Figure 13.4 (trace b) and a simulation of the same data (trace a). The row corresponds to the row of peaks at the bottom of the spectrum (highest frequency in F_1). The spectrum was simulated using the SIMPLTN program which provides an exact density matrix calculation.

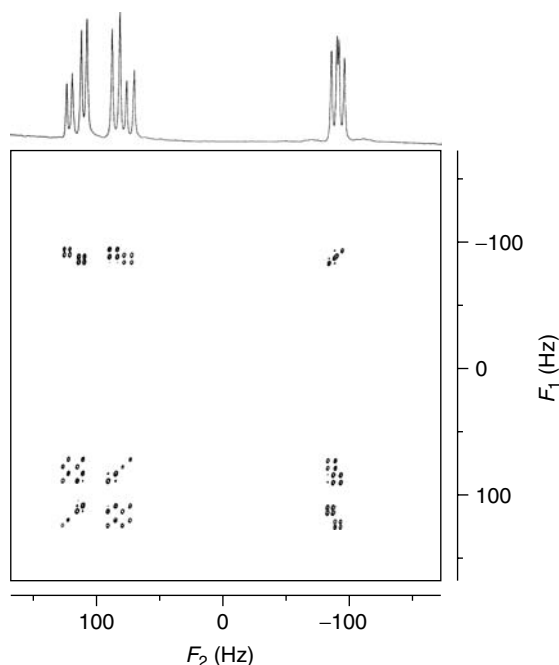


Figure 13.7. Magnitude calculation COSY on serine at 500 MHz, but with a mixing pulse of $\pi/4$. All other parameters are as in Figures 13.4 and 13.6.

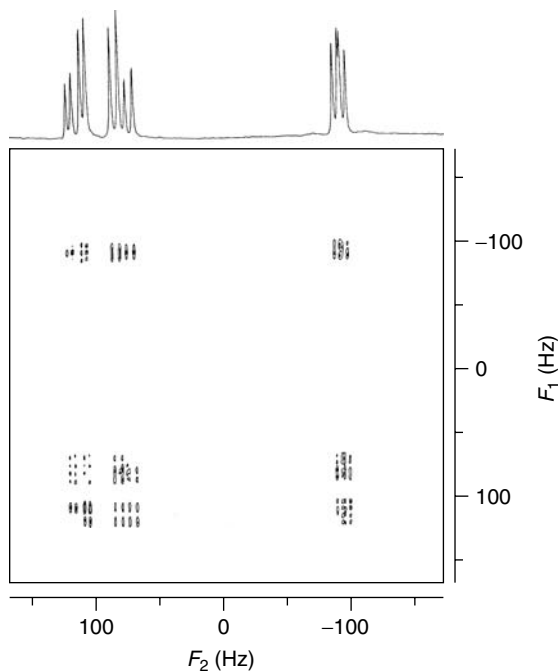


Figure 13.6. Magnitude calculation COSY on the same serine sample as in Figure 13.4, also with a mixing pulse of $\pi/2$ but at 500 MHz. The spectral width and the number of experiments is the same as in Figure 13.4.

protons can be easily manipulated by changing the pH of the solution.

Two other solutions to the quadrature detection problem keep the pure phase lineshapes. One is effectively to move $F_1=0$ through the use of the time proportional phase increment (TPPI) and still use a real FT.¹¹ The other method is to collect a parallel data set that is phase-shifted, so that there is true complex data in both dimensions. In this case, a complex FT can be used in both domains.¹² Both methods are widely used and except for some minor details in the baseline the two are essentially equivalent.¹³

The final problem is to make all of the lines, both cross peaks and diagonal peaks, the same phase. If we use a double quantum filter in the mixing pulse,^{14,15} this achieves the goal of a homonuclear correlation with pure absorption lines.

For the analysis of the fine structure within a multiplet, the COSY experiment with phase sensitive transforms and double quantum filtering is the method of choice. For quick, qualitative experiments to determine a rough connectivity network, the magnitude

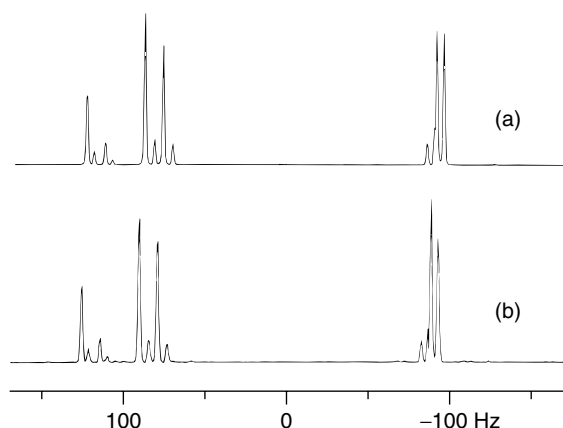


Figure 13.8. Plot of the row of peaks at the bottom (highest F_1 frequency) of the 2D spectrum in Figure 13.7 [trace (b)]. Trace (a) represents a SIMPLTN simulation of the data.

calculation COSY is quicker to set up and process (in fact it can easily be set up automatically by the spectrometer). Depending on what sort of information is required, one of these two experiments is used in most cases.

13.2.6 Intensities of Cross Peaks and Digitization Effects

The fact that the two elements in the cross peak in equations (13.5) and (13.6), are of opposite sign is a general one: the cross peaks always have zero net intensity if the acquisition begins immediately after the mixing pulse. For a weakly coupled AX system as above, the ratio of the peaks is 1:−1. For more complex multiplets, the relative intensities can be built up from the AX case as for 1D spectra. For equivalent spins, Pascal's triangle can be used so that for the cross peak in an AX_2 system the ratios of the peaks are 1:0:−1 and the peaks in an AX_3 system are in the proportion of 1:1:−1:−1. These ratios will be evident in a phase sensitive COSY, but a magnitude calculation COSY will mask the signs of the peaks.

In a more complex spin system, the distinction between active and passive couplings becomes important. Within a given set of cross peaks, representing the correlation between spin A and spin X, the

J_{AX} is the active coupling. This coupling will appear as an antiphase arrangement, as above, but all the other couplings will appear as normal. The splitting due to coupling from A to another spin, M, will appear in phase within the AX cross-peak group. Of course, in the cross-peak group joining A and M, then J_{AM} will be the active coupling.

As the coupling approaches zero the cross peak should vanish, so the net cross-peak intensity must be zero. However, adding a delay after the mixing pulse before the start of the acquisition will enhance cross peaks due to long-range coupling. This delay should be some fraction of the coupling, so that the peaks that are exactly out of phase after the mixing pulse have some time to approach being in phase. Similarly, a delay before the mixing pulse will allow multiplets time to get out of phase and enhance polarization transfer. If these delays are present, then the cross peak will acquire some net intensity and cross peaks due to quite small couplings will be evident in the 2D spectrum.¹⁶

Similarly, poor digitization should cause cross peaks to disappear. If the digitization is such that a single point in two dimensions represents an entire set of cross peaks due to two multiplets, that point should have zero intensity. Very good digitization should give accurate intensities. In between these extremes, however, the behavior is somewhat unusual. When the digitization (in Hz per point) approaches the value of the coupling constant J (in Hz), simulations show that the apparent intensity of the cross peak rises rather than falls. The apparent intensity reaches a maximum at a ratio of $J/\text{digitization}$ of approximately 1, and there is still significant intensity when the coupling is only 0.2 of the digitization.¹⁷ This effect, combined with the possible use of fixed delays around the mixing pulse, permits us to use quite small data matrices and still see useful correlations.

Provided digital resolution is not a problem, the cross peak between an A spin and an X spin will be as follows. If it is the peak in F_1 which corresponds to the A frequency in F_2 , then the rows will resemble the A spectrum and the columns the X spectrum, as shown in Figure 13.4. Similarly, the other cross peak will resemble the X spectrum along the F_2 rows and the A spectrum in F_1 . The only difference will be that the splittings due to the A–X coupling will appear as an antiphase, 1:−1, orientation, but all other couplings will be normal.

13.2.7 Flip Angle Effects

If we use the simple trigonometric identity given in equation (13.8), we can see from equation (13.3) that three of the lines in the simple two-spin COSY behave identically with respect to the flip angle of the mixing pulse. The odd line is the off-diagonal member of the diagonal group of peaks—the peak due to mixing of one line with the other line in the doublet. In Figure 13.2, we can observe that these are the only pairs of transitions that do not share at least one energy level. All other peaks in the 2D spectrum come from pairs of “connected” transitions.

$$\sin^2 \alpha = 2 \sin^2 \frac{\alpha}{2} (1 + \cos \alpha) \quad (13.8)$$

Equation (13.3) predicts that this peak from “unconnected” transitions will decrease in intensity relative to the others as the flip angle of the mixing pulse is decreased. For a flip angle of $\pi/4$, this peak is approximately 17% of the others. Judicious choice of a contour level in the plot of a 2D spectrum will make this peak disappear, so the diagonal region of the spectrum is much cleaner. This is shown by comparing Figures 13.6 and 13.7. As Figure 13.8 shows, the peaks do not disappear.

Another consequence of this shows up in the cross peaks of bigger spin systems. Here also there are peaks due to pairs of unconnected transitions. Depending on the relative signs of couplings, this gives a characteristic “tilt” to the cross peak. This can be used to assign the relative signs of couplings. In an AMX spin system, the tilt of the cross peak between A and M will indicate the relative signs of J_{AX} versus J_{MX} . Figures 13.6 and 13.7 show this effect for serine. The cross peak between the two β protons at the high-frequency side of the spectrum tilts one way, since the couplings to the third (α) proton are both vicinal and of the same sign. However the α – β cross peaks tilt the other way because of the opposite signs of the vicinal and geminal couplings.

The use of a different flip angle for the mixing pulse will decrease the intensity of these peaks but it will not eliminate them, as shown in Figures 13.7 and 13.8. If the peaks are to be eliminated, then another variation of the simple experiment, E.COSY, should be used¹⁸ (see Chapter 14). This is more complex to set up, but it will give more reliable and useful intensities. This will be useful, for example, in the automatic interpretation of COSY spectra.

13.2.8 Strong Coupling Effects

Most homonuclear spin systems show some signs of strong coupling. This is more evident in the intensities of the lines rather than in the line positions. This is because the intensities of the lines are determined by the xy magnetizations of the spin system, which are perturbed to first order by strong coupling. The line positions depend on the energy levels and z magnetizations, which are perturbed only to second order. The general rule that no new frequencies will appear in F_1 in COSY still holds. However, since the COSY experiment involves the mixing of xy magnetizations it is clear that intensities will be greatly affected by strong coupling.

As an example, let us consider a magnitude calculation COSY on a simple AB spin system. In such a system, we need only consider the negative frequency coherences, as in equation (13.2), and how much is transferred to the positives for detection, as in equation (13.5). For such a system, it is convenient to define the frequencies of the four lines in the spectrum in the following way. Let ν_0 be the average of the A and B Larmor frequencies, and let δ be the difference of the Larmor frequencies in Hz. If J is the scalar coupling constant between A and B, then we can define $C = (J^2 + \delta^2)^{1/2}$ and an angle, θ , by the relationship $\sin(2\theta) = J/C$. For simplicity of notation, let $c = \cos(\theta)$ and $s = \sin(\theta)$. For simplicity, let us number the frequencies as in equation (13.9).

$$\left. \begin{aligned} \nu_1 &= \nu_0 + C/2 + J/2 \\ \nu_2 &= \nu_0 + C/2 - J/2 \\ \nu_3 &= \nu_0 - C/2 + J/2 \\ \nu_4 &= \nu_0 - C/2 - J/2 \end{aligned} \right\} \quad (13.9)$$

With these definitions, we can calculate the evolution of the negative frequencies up to the mixing pulse, as in equation (13.2), to give equation (13.10).

$$\left. \begin{aligned} |- \nu_1) &= (c - s)e^{-i(\nu_0 + C/2 + J/2)t_1} \\ |- \nu_2) &= (c + s)e^{-i(\nu_0 + C/2 - J/2)t_1} \\ |- \nu_3) &= (c + s)e^{-i(\nu_0 - C/2 + J/2)t_1} \\ |- \nu_4) &= (c - s)e^{-i(\nu_0 - C/2 - J/2)t_1} \end{aligned} \right\} \quad (13.10)$$

Note that the coherences do not have equal intensity as was the case in the weakly coupled spin system.

Let us only consider the case of a flip angle of the mixing pulse of $\pi/2$, in order to simplify the calculation somewhat. Using published methods,^{19,20} it is relatively easy to show that the effect of the mixing pulse on the coherences in equation (13.10) is given by the matrix in equation (13.11). This is

the strong-coupling equivalent of equation (13.3) for a flip angle of $\pi/2$.

$$\frac{1}{4} \begin{bmatrix} (c-s)^2 & c^2-s^2 & c^2-s^2 & -(c+s)^2 \\ c^2-s^2 & (c+s)^2 & -(c-s)^2 & c^2-s^2 \\ c^2-s^2 & -(c-s)^2 & (c+s)^2 & c^2-s^2 \\ -(c+s)^2 & c^2-s^2 & c^2-s^2 & (c-s)^2 \end{bmatrix} \quad (13.11)$$

Finally, strong coupling also implies that not all lines are detected with equal intensity. This means that the final intensities are the result of multiplying the coherences in equation (13.10) by the matrix in equation (13.11) and then multiplying by the detection efficiency, as in equation (13.12).

$$\left. \begin{aligned} |v_1\rangle &= \frac{1}{4}(c-s)[(c-s)^2(c-s)e^{-iv_1t_1} \\ &\quad + (c^2-s^2)(c+s)e^{-iv_2t_1} \\ &\quad + (c^2-s^2)(c+s)e^{-iv_3t_1} \\ &\quad - (c+s)^2(c-s)e^{-iv_4t_1}] \\ |v_2\rangle &= \frac{1}{4}(c+s)[(c^2-s^2)(c-s)e^{-iv_1t_1} \\ &\quad + (c+s)^2(c+s)e^{-iv_2t_1} \\ &\quad - (c-s)^2(c+s)e^{-iv_3t_1} \\ &\quad + (c^2-s^2)(c-s)e^{-iv_4t_1}] \\ |v_3\rangle &= \frac{1}{4}(c+s)[(c^2-s^2)(c-s)e^{-iv_1t_1} \\ &\quad - (c-s)^2(c+s)e^{-iv_2t_1} \\ &\quad + (c+s)^2(c+s)e^{-iv_3t_1} \\ &\quad + (c^2-s^2)(c-s)e^{-iv_4t_1}] \\ |v_4\rangle &= \frac{1}{4}(c-s)[- (c+s)^2(c-s)e^{-iv_1t_1} \\ &\quad + (c^2-s^2)(c+s)e^{-iv_2t_1} \\ &\quad + (c^2-s^2)(c+s)e^{-iv_3t_1} \\ &\quad + (c-s)^2(c-s)e^{-iv_4t_1}] \end{aligned} \right\} \quad (13.12)$$

Equation (13.12) shows the intensities of all the lines in a COSY spectrum of an AB spin system. If we apply the trigonometric identities in equation (13.13), we can further simplify the expressions.

$$\left. \begin{aligned} \cos^2 \theta - \sin^2 \theta &= \cos 2\theta \\ (\cos \theta + \sin \theta)^2 &= (1 + \sin 2\theta) \\ (\cos \theta - \sin \theta)^2 &= (1 - \sin 2\theta) \end{aligned} \right\} \quad (13.13)$$

The final expressions for the COSY on an AB system are given in equation (13.14).

$$\left. \begin{aligned} |v_1\rangle &= \frac{1}{4}[(1 - \sin 2\theta)^2 e^{-iv_1t_1} + \cos^2 2\theta e^{-iv_2t_1} \\ &\quad + \cos^2 2\theta e^{-iv_3t_1} - \cos^2 2\theta e^{-iv_4t_1}] \\ |v_2\rangle &= \frac{1}{4}[\cos^2 2\theta e^{-iv_1t_1} + (1 + \sin 2\theta)^2 e^{-iv_2t_1} \\ &\quad - \cos^2 2\theta e^{-iv_3t_1} + \cos^2 2\theta e^{-iv_4t_1}] \\ |v_3\rangle &= \frac{1}{4}[\cos^2 2\theta e^{-iv_1t_1} - \cos^2 2\theta e^{-iv_2t_1} \\ &\quad + (1 + \sin 2\theta)^2 e^{-iv_3t_1} + \cos^2 2\theta e^{-iv_4t_1}] \\ |v_4\rangle &= \frac{1}{4}[-\cos^2 2\theta e^{-iv_1t_1} + \cos^2 2\theta e^{-iv_2t_1} \\ &\quad + \cos^2 2\theta e^{-iv_3t_1} + (1 - \sin 2\theta)^2 e^{-iv_4t_1}] \end{aligned} \right\} \quad (13.14)$$

The true diagonal peaks show the expected behavior: the result of mixing a line with itself gives the square of the intensity in the 1D spectrum. However, all the other peaks show the same intensity, even as a result of mixing one low-intensity outer peak with the other outer peak. This is somewhat unexpected, but is shown experimentally in the spectra of serine in Figures 13.4 and 13.5.

13.3 LARGER SPIN SYSTEMS

Larger spin systems can be treated as simple combinations of two-spin systems in most cases. The cross peaks will reflect the structures of the F_1 and F_2 spectra as above, with the proviso about the active coupling being in antiphase. Provided the system is in equilibrium, there will be no new frequencies appearing in F_1 . In strongly coupled systems, the intensities of some individual peaks may be such that they are missing from a contour plot, but a cross peak will still be visible. Some spin systems, such as the ABX system, can be analyzed algebraically, but the calculations can get quite complex even for a simple experiment like COSY. For these systems, computer simulations provide a very useful tool.²¹⁻²⁵ With modern computers, exact density matrix calculations can be done in a few minutes on systems of four or five strongly coupled spins. For example, the simulations for Figures 13.5 and 13.8 were undertaken in under 30 s on a 1992 model UNIX workstation. For systems with several spins, a combination of the basic rules for two spins and some simulations and experience will faithfully predict the quantitative nature of the COSY spectrum.

13.4 FAST PULSING ARTIFACTS

The statement that no new frequencies appear in a COSY rests on the assumption that the spins relax completely between pulse sequences, and this is almost never true in practice. Under normal circumstances, artifacts that are derived from the F_2 frequencies will appear in the spectrum. Usually these appear as peaks at $F_1 = 0$, small P-type peaks which have not been totally suppressed or peaks at multiples of the F_2 frequency. These are especially evident for strong singlets due to methyl groups, which often have long relaxation times. These artifact peaks can

be minimized by doing dummy scans before the actual acquisition, in order to get the spin system into a steady state. Also, careful attention to the phase cycling sequence and how one experiment interacts with the next can be very helpful.^{26,27} Also, the use of magnetic field gradients, rather than phase cycling, to select coherence pathways is very effective in reducing the artifacts due to incomplete relaxation.

13.5 CONCLUSIONS

The COSY experiment serves as the best example of two-dimensional NMR spectroscopy. In its many forms it is an extraordinarily useful experiment, and yet it is quite simple to analyze and understand. The two-spin systems described here illustrate almost all the important features of the experiment. A few pages suffice to describe these systems completely and quantitatively, so it is well within the reach of all NMR spectroscopists. This combination of simplicity and power makes the COSY experiment stand out.

RELATED ARTICLES IN THE ENCYCLOPEDIA OF MAGNETIC RESONANCE

**Analysis of High-Resolution Solution
State Spectra**

Phase Cycling

Radiofrequency Pulses: Response of Nuclear Spins

REFERENCES

1. W. P. Aue, E. Bartholdi, and R. R. Ernst, *J. Chem. Phys.*, 1976, **64**, 2229.
2. K. Nagayama, K. Wüthrich, and R. R. Ernst, *Biochem. Biophys. Res. Commun.*, 1979, **90**, 305.
3. A. D. Bain, R. A. Bell, J. R. Everett, and D. W. Hughes, *J. Chem. Soc., Chem. Commun.*, **1980**, 256.
4. O. W. Sørensen, G. W. Eich, M. H. Levitt, G. Bodenhausen, and R. R. Ernst, *Prog. Nucl. Magn. Reson. Spectrosc.*, 1983, **16**, 163.
5. A. D. Bain, *Prog. Nucl. Magn. Reson. Spectrosc.*, 1988, **20**, 295.
6. A. D. Bain, I. W. Burton, and W. F. Reynolds, *Prog. Nucl. Magn. Reson. Spectrosc.*, 1994, **26**, 59.
7. S. Boentges, B. U. Meier, C. Griesinger, and R. R. Ernst, *J. Magn. Reson.*, 1989, **85**, 337.
8. A. D. Bain, *J. Magn. Reson.*, 1988, **77**, 125.
9. A. D. Bain, *J. Magn. Reson.*, 1984, **56**, 418.
10. G. Bodenhausen, H. Kogler, and R. R. Ernst, *J. Magn. Reson.*, 1984, **58**, 370.
11. D. Marion and K. Wüthrich, *Biochem. Biophys. Res. Commun.*, 1983, **113**, 967.
12. D. J. States, R. A. Haberkorn, and D. J. Ruben, *J. Magn. Reson.*, 1982, **48**, 286.
13. J. Keeler and D. Neuhaus, *J. Magn. Reson.*, 1985, **63**, 454.
14. U. Piantini, O. W. Sørensen, and R. R. Ernst, *J. Am. Chem. Soc.*, 1982, **104**, 6800.
15. A. J. Shaka and R. Freeman, *J. Magn. Reson.*, 1983, **51**, 169.
16. A. Bax and R. Freeman, *J. Magn. Reson.*, 1981, **44**, 542.
17. T. Allman and A. D. Bain, *J. Magn. Reson.*, 1986, **68**, 533.
18. C. Griesinger, O. W. Sørensen, and R. R. Ernst, *J. Chem. Phys.*, 1986, **85**, 6837.
19. A. D. Bain, *Chem. Phys. Lett.*, 1978, **57**, 281.
20. L. E. Kay and R. E. D. McClung, *J. Magn. Reson.*, 1988, **77**, 258.
21. P. Meakin and J. P. Jesson, *J. Magn. Reson.*, 1975, **18**, 411.
22. B. K. John and R. E. D. McClung, *J. Magn. Reson.*, 1984, **58**, 47.
23. H. Widmer and K. Wüthrich, *J. Magn. Reson.*, 1986, **70**, 270.
24. W. Studer, *J. Magn. Reson.*, 1988, **77**, 424.
25. A. Majumdar and R. V. Hosur, *Prog. Nucl. Magn. Reson. Spectrosc.*, 1992, **24**, 109.
26. C. J. Turner and S. L. Patt, *J. Magn. Reson.*, 1989, **85**, 492.
27. C. J. Turner and W. C. Hutton, *J. Magn. Reson.*, 1992, **100**, 469.